

SLOVAK OPTICAL TELESCOPE AND IMAGE PROCESSING PIPELINE FOR THE SPACE DEBRIS AND NEA OBSERVATIONS AND RESEARCH

J. Šilha⁽¹⁾, S. Krajčovič⁽¹⁾, D. Žilková⁽¹⁾, J. Világi⁽¹⁾, F. Ďuriš⁽¹⁾, V. Nagy⁽¹⁾, J. Tóth⁽¹⁾, M. Trujillo⁽²⁾, and T. Flohrer⁽³⁾

⁽¹⁾*Faculty of Mathematics, Physics and Informatics, Comenius University in Bratislava, Slovakia, Email: jiri.silha@fmph.uniba.sk*

⁽²⁾*ESA/ESTEC, Keplerlaan 1, PO Box 299, NL-2200 AG Noordwijk, The Netherlands*

⁽³⁾*ESA/ESOC, Space Debris Office, Robert-Bosch-Strasse 5, DE-64293 Darmstadt, Germany*

ABSTRACT

Slovakia became the 9th ESA European Cooperative State in 2015. The Department of Astronomy and Astrophysics (DAA), Faculty of Mathematics, Physics and Informatics of Comenius University in Bratislava, Slovakia (FMPI CU) was granted resources from the first ESA PECS call to action to transform a 0.7m Newton telescope used for amateur observations into a professional optical system capable of tracking space debris and other naturally formed objects. An another part of this activity was to develop a software (in coordination with the Department of Applied Informatics, FMPI CU) that would handle and process images yielded by the newly acquired telescope.

In this paper, we present in total 9 Image Processing Elements (IPEs) that are currently being used as a pipeline at the Astronomical and Geophysical Observatory in Modra, Slovakia (AGO) to track, classify and identify space debris objects. We employ many state of the art and experimental algorithms aimed to provide efficient and high quality results with the available technology.

Keywords: space debris; optical measurements; image processing; software development.

1. INTRODUCTION

Humanity has long been able to put both manned and unmanned vehicles into space to perform various missions focused on advancing the understanding of the world outside our home planet and achieving technological progress which would not be possible otherwise.

However, it all comes at a cost in the form of space debris. Either it is inefficient to return the sent satellites back home or they stop to function naturally, we see a steep increase in artificial non-functional objects orbiting around Earth. Although the major national (e.g. NASA)

or international (e.g. ESA) agencies already have plans in place to mitigate this growing danger, it is still vital to track and catalogue existing debris.

In order to understand space debris, we must firstly categorize it into separate groups from multiple angles. The first useful division is according to its type. For further information, see [1].

The second classification would be according to an object's size - small debris and large debris. Both of these groups are dangerous in its own ways - either as a swarm of sub-centimetre particles or a single few metres long object - and are still a threat to the currently ongoing and future missions. Size distinction is crucial for tracking because the small objects are virtually invisible from the Earth's surface and require the use of radars or space-based telescopes placed on low Earth orbit (LEO).

Large objects are most usually tracked by the use of optical telescopes, which are generally placed at high altitudes with minimal light pollution and good atmospheric conditions. Astronomical night, when the Sun is more than 18° below the horizon, and the tracked objects are still illuminated, is the main requirement for the operation of such devices. Refractors (using lens systems) and reflector (using mirror surfaces to focus incoming light) telescopes have each their own uses, pros and cons. Based on the same principle of collecting photons which were reflected or emitted by a space object, the light is translated into an image with additional information and used for further processes [1]. Acquiring an image is therefore only a small part of the whole pipeline, nevertheless one of the most important ones.

2. PIPELINE OVERVIEW

The concept of complex image processing pipelines with the objective of sky surveys is not new - see ESA OGS [2], Apex II [3] or Pan-STARRS [4]. However, in this section, we describe our image processing pipeline which

was inspired with the aforementioned systems - its elements and algorithms - in greater detail. This pipeline is deployed at the Astronomical and Geophysical Observatory in Modra, Slovakia (AGO).

2.1. AGO image processing pipeline

AGO uses its own optical sensors. Primarily, the pipeline has been developed for a Newton telescope with a very thin 700 mm parabolic Alluna optics mirror supported by a gravity actuator (AGO70) [5] (see Figure 1).



Figure 1. Newton telescope with a 700 mm parabolic mirror situated at the Astronomical and Geophysical Observatory in Modra, Slovakia.

In total, there are 9 image processing elements (IPEs) in the pipeline, each with its own role:

1. star field identification,
2. image reduction,
3. background estimation and subtraction,
4. objects search and centroiding (segmentation),
5. astrometric reduction,
6. masking,
7. tracklet building,
8. object identification,
9. data format transformation.

Figure 2 shows the simplified diagram demonstrating the data flow between each IPE. The whole procedure starts with an acquisition of a raw scientific (LIGHT) frame/image ("Image 1") which is sent to the star field identification IPE. Then the frame is updated with information about the center of field-of-view ("Image 2"), is reduced by subtracting master DARK (acquired with same the exposure time as is the scientific frame) and master FLAT FIELD frames used from the internal archive. The background is estimated and subtracted

from "Image 3" and then the resulting "Image 4" is processed with the objects search and centroiding algorithm. The output of previous process is a series of frame objects identified in the frame ("Data 1"), including the stars. "Data 1" is sent to astrometric reduction where the plate constants are found and to each frame object is associated its astrometric position ("Data 2"). The whole data set is then screened by masking IPE, which removes the majority of the star frame objects. Once screened, "Data 3" are used for tracklet building. The output is a series of tracklets "Data 4" which is then compared with a TLE catalogue for identification. Once the object is identified, "Data 5" is converted from internal format to the required data format ("Data 6").

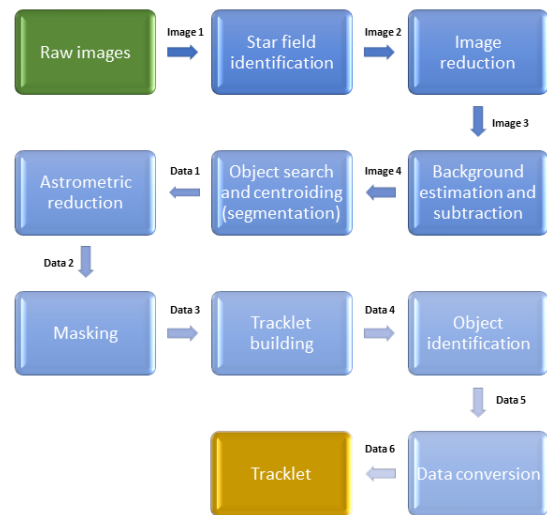


Figure 2. Simplified diagram demonstrating the interactions and data flows between FMPI's Image Processing Elements (IPEs) used for the AGO70 telescope pipeline for the astrometric and photometric reductions.

2.2. Image reduction

The goal of this IPE is to remove additive and multiplicative errors from the captured raw image. Additive errors are caused by bias and dark currents, while multiplicative errors are caused by illumination differences, a different quantum efficiency of pixels, or dust halos. Removal of additive errors is done by creating a DARK frame (taken at a specific exposure time to capture the dark current in pixels) or a BIAS frame (taken at zero exposure time) and subtracting it from the original image. A FLAT FIELD frame is created by taking images both at dusk and at dawn, close to the zenith direction, on an evenly illuminated field; it is further used to remove multiplicative errors.

Our image reduction IPE is responsible for following steps:

1. creating a master frame for DARK or BIAS, either

by using average (mean) or median values of pixels' intensity,

2. creating a master frame for FLAT FIELD, either by using average (mean) or median values of normalized pixels' intensity,
3. subtracting the master DARK and/or BIAS calibration frame from the LIGHT frame,
4. dividing the LIGHT frame by the master FLAT FIELD frame.

Output of this step is a reduced image, free from additive and multiplicative errors.

2.3. Background estimation

This IPE is used to further modify the acquired image by estimating the background noise and therefore differentiating between real objects and the noise.

We use subsequent sigma clipping [3] to perform this task. The first step of this algorithm is to shrink the image to 10% of its size by a spline filter to minimize the aliasing effect. Next, we smooth the image by a median filter. There are several methodologies of acquiring the filter, either by taking the median value of all pixels or by using the smallest median of all sub-frames of the main frame. The image is then enlarged to its original size. Sigma clipping is performed iteratively by examining each pixel of the image. If the intensity of the given pixel is larger than 3σ we replace the intensity by the previously obtained median value. If it is smaller, we ignore this pixel and move onto the next one. While being fast, this algorithm has a disadvantage of removing faint objects.

Output of this step is a series of two images - one containing the estimated background map and second the modified image corrected by the background map. Example of original image, estimated background and their difference can be seen in Figure 3.

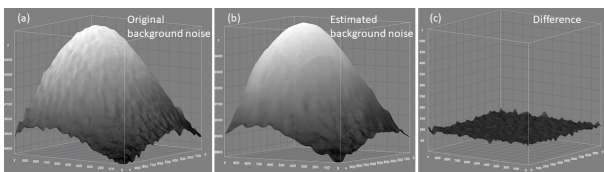


Figure 3. The 3D-surface plot of original background noise frame (a), estimated background noise frame by using the IPE background estimation (b), and both frames subtracted (c). Images generated by the AstroImageJ tool [6].

2.4. Objects search and centroiding

This IPE consists of three separate parts: search algorithm, centroiding algorithm, and touch-down algorithm.

The search algorithm's role is to find pixels in the frame which are above a defined threshold that depends on the background level and frame objects' signal-to-noise-ratio (SNR).

The centroiding algorithm is responsible for measuring the frame object's position (its centroid or center-of-mass) and the total intensity of the frame object. Prerequisite of this step is the found pixels from the previous step and a size of a rectangle which is to be fitted onto the frame object.

The touch-down algorithm is an iterative procedure performed to refine the previous step and calculate a better center position of the object. If the difference between the previously calculated center and the currently calculated center is larger than a defined threshold, the center is moved and another iteration is performed. If not, we have successfully found a center of the frame object and its centroid.

An example of processed frame can be seen in Figure 4. The original frame along with the detected frame objects are shown in the left hand side and comparison of observed minus calculated (O-C) values for the centroids' positions is shown on the right hand side of the image.

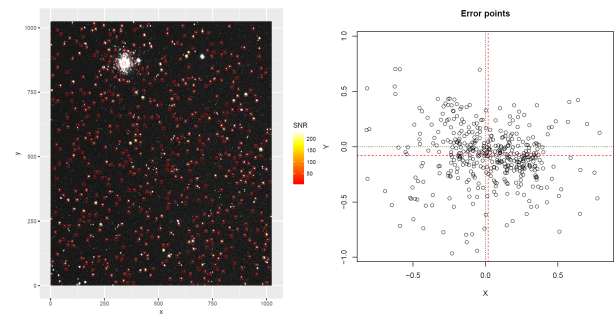


Figure 4. Figures generated by the IPE objects search and centroiding. In the left we show original frame with detected frame objects marked by a square. In the right we show observed minus calculated (O-C) centroids' positions.

We validated the IPE on real and synthetic frames by focusing on the detection efficiency of the algorithm and position accuracy. The results for 9 different frames can be seen in Figure 5. We distinguish between frames containing stars as points (sidereal tracking) and frames representing stars as streaks (GEO tracking). The test cases revealed that the detection efficiency is quite low, around 50% while the centroids accuracy reached values around 0.1 arcsec.

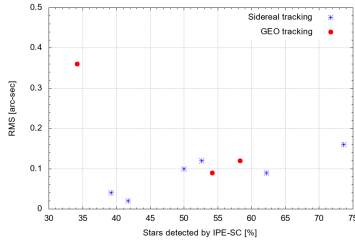


Figure 5. Detection efficiency (horizontal axis) versus measured accuracy (vertical axis) of the IPE objects search and centroiding.

2.5. Star field identification

Star field identification IPE is based on scripts provided by the Astrometry.net [7] and is automatically called by the system at our server when the image is acquired. It is responsible for finding the center of field-of-view in right ascension and declination coordinates, done by scripts performing segmentation and then astrometric reduction. The FITS file's header is then extended by the obtained data - center of field-of-view, "RA" as the keyword for right ascension, "DEC" as the keyword for declination, and plate constants.

2.6. Astrometric reduction

While using the same scripts (Astrometry.net) as the previous IPE, astrometric reduction has a different input, output and the segmentation function is replaced by IPE objects search and centroiding (see subsection 2.4).

There are two main steps which are done in order to perform this IPE successfully:

1. find the plate constants solutions,
2. transform the coordinates and update the input file for RADEC coordinates.

As mentioned before, values of plate constants are calculated using Astrometry.net. A TSV file (generated by IPE objects search and centroiding (see subsection 2.4)) is needed as an input. IPE reads the frame coordinates (x, y) , finds the plate constants by using Astrometry.net and transform coordinates (x, y) into the J2000 equatorial coordinates. The TSV file is then appended with the calculated values.

We used five test FITS frames for astrometric reduction validation. Two of such frames are plotted in Figure 6. We show a highly dense star field (approx. 630 stars) and synthetically generated star field with stars as streaks. All five frames have been processed with the Astrometrica tool [8] first, which we used as a reference, and then with our IPEs objects search and centroiding (section 2.4) and

astrometric reduction. For both processes we calculated residuals (RMS) by comparing the star catalogue positions with measured positions. The results can be seen in Figure 7 where RMS values in [arcsec] are plotted. In general, the RMS are higher for our IPE (from 0.79 - 1.55 arcsec) than for Astrometrica solutions (from 0.21 - 0.62 arcsec).

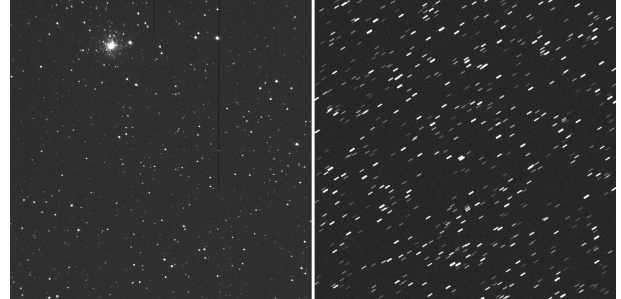


Figure 6. Examples of two FITS frames used for the astrometric reduction validation. Frames 2017_PR25_R_3038_df.fits and 3869_R_2013_gen_s.fits are plotted.

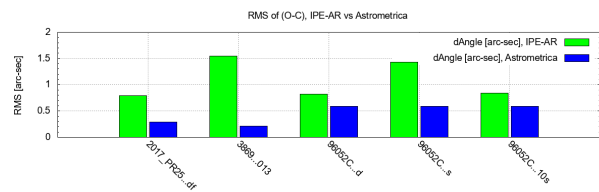


Figure 7. RMS values of (O-C) as calculated by IPE-AR and Astrometrica. Plotted is total angular distance in [arcsec].

2.7. Masking

Masking (data screening) removes objects in close proximity on series of textual data from images. It is crucial to identify star frame objects - this is done by assuming that all source images in the series have similar star field. We then compare the J2000 coordinates of frame objects measured at different times. For example, if interested in geocentric objects, objects which have angular velocity lower than 1 arcsec/s are considered stars and removed from the textual data. To calculate angular velocity we use the cosine rule to get the angular distance of two points on the sphere. We use cosine rule as follows:

$$threshold < \cos^{-1}(\sin \delta_i \sin \delta_j + \cos \delta_i \cos \delta_j \cos(\alpha_j - \alpha_i))$$

The principle of the IPE masking is demonstrated in Figure 8. While points $\{1, 5\}$, $\{3, 7\}$, $\{4, 8\}$ represent three stars (left frame), point $\{2, 6\}$ represents our object of interest. Because the apparent motion for the stars between

the two frames was less than defined threshold (marked as cone in the figures) they were removed from the data set (right). From our experience with data acquired by the AGO70, the most reliable threshold for filtering stars is 6 arcsec/s.

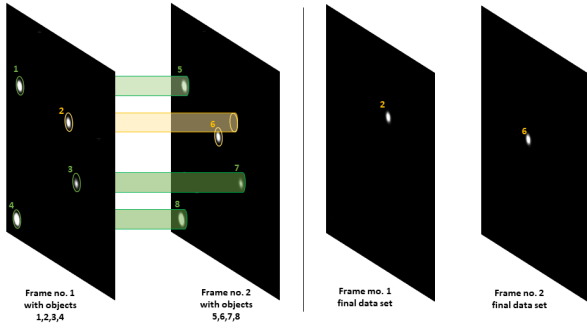


Figure 8. Star objects identification principle used during the IPE masking. The width of the cone represents the defined threshold.

Yet another filter used to further thin out non-realistic frame objects which can be either cosmic or very bright pixels is a simple if clause removing all detected objects with total intensity lower than 100 ADU.

After the masking is applied the screened TSV file is generated for further processing.

Validation of the IPE masking on 20 different series each containing at least 8 frames and acquired either by using sidereal tracking, GEO tracking or object tracking showed that this algorithm works very reliably, detecting and removing more than 75% of all stars from the series. This dramatically decreases processing during the next step, tracklet building.

2.8. Tracklet building

First and foremost, it is important to define what a tracklet is. The most used definition is that it is a *data structure containing consecutive observations of a frame object in time*. Simply said, tracklet roughly represents measurements of a portion of the trajectory of an object.

The main premise is that the field-of-view is small enough that objects' orbits appear to move according to linear motion - they move along a line and have close to zero acceleration [9]. Keeping this fact in mind, we use simple linear regression algorithm to create lines and predict tracklets. Linear regression is a well-known statistical concept modelling the linear relationship between a scalar dependent variable y and a scalar independent variable x .

We have m number of frames and $n_1 \dots n_m$ number of frame objects defined by a measurement point $p_{ki}(\alpha_{ki}, \delta_{ki}, t_{ki})$ where k stands for k -th frame. The

first step is pairing each unknown point $p_{1i}(\alpha_{1i}, \delta_{1i}, t_{1i})$ from the first frame acquired at epoch t_1 with each unknown point $p_{2j}(\alpha_{2j}, \delta_{2j}, t_{2j})$ from the second frame acquired at epoch t_2 . Then we create a line l_{1i2j} such that $p_{1i}, p_{2j} \in l_{1i2j}$. The final number of existing lines after this procedure is equal to the number of all unknown objects from the first frame n_1 multiplied by the number of all unknown objects from the second frame n_2 . It can be relatively high - this depends on the quality of pre-processing of each image. The next step is to iterate over the remaining "images" (keep in mind that we work with textual data) and to filter out points which are too far from the line. The points which fall under a defined threshold representing the distance from the line are further considered to be part of the currently constructed tracklet by a weighing algorithm. The weights are assigned to each point by firstly calculating apparent angular velocity $\omega_{radec,1i,2j}$ and position angle $PA_{radec,1i,2j}$ which are considered as a *baseline*. Secondly, we calculate the apparent angular velocity $\omega_{radec,ki,k+cj}$ and position angle $PA_{radec,ki,k+cj}$ where $c < n$ for all remaining frames. Points which are closer to the *baseline* have a bigger weight and have a higher probability of being the objects we are searching for and therefore included in the tracklet.

To successfully create a tracklet, at least four confirmed observation points are required. All valid tracklets are stored in a file in our own internal format.

We tested the IPE tracklet building on 20 series each with at least 8 frames. We acquired series for NEA, GEO and Molniya objects. The number of frame objects per series varied accordingly to the star field density and efficiency of the IPE masking discussed in the previous section. This can be seen in Figure 9.

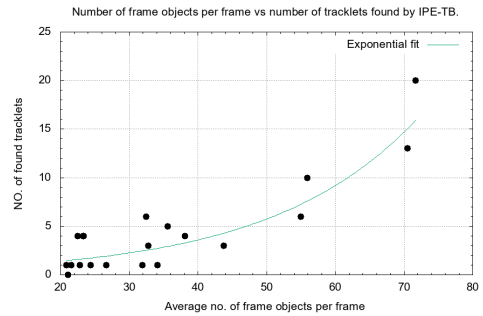


Figure 9. Number of tracklets found by IPE tracklet building as a function of average number of frame objects per frame.

2.9. Object identification

After successfully creating a tracklet, we need to correlate the observations in it with a catalogue to identify which object we were observing. There are three parameters which are used to do this - namely angular distance θ , position angle PA and angular velocity ω .

Positions of catalogued objects are determined by using SGP model [10] and TLE data from the catalogue, which can be either public (from www.space-track.org), or internal (Astronomical Institute of University Bern (AIUB)/ESA catalogue). At first, we calculate parameters θ_c , PA_c , and ω_c where the subscript c denotes that they belong to the catalogued object. Then, we determine parameters for the tracklet - θ_t , PA_t , ω_t and compare them with the parameters for catalogued objects. By reasonably defining threshold for each of these parameters, $\theta_{threshold}$, $PA_{threshold}$, $\omega_{threshold}$ we correlate the tracklet with an object from the catalogue.

2.10. Data format transformation

This IPE is responsible for conversion of astrometric positions from our own internal tracklet format to Consultative Committee for Space Data Systems (CCSDS) Tracking Data Message (TDM) [11], AIUB's OBS, and Minor Planet Center (MPC) format. Additionally, the photometric measurements are converted to the Inter-Agency Space Debris Coordination Committee (IADC) light curve format.

3. SUMMARY

In our work we present our modular image processing pipeline largely developed by the Faculty of Mathematics, Physics and Informatics of Comenius University in Bratislava, Slovakia (FMPI CU) for our 0.7-m Newton telescope (AGO70). This work brings FMPI CU closer to a semi-automated image processing of space debris and NEA measurements which is crucial for increasing the system efficiency.

Presented pipeline consists from nine independent image processing elements (IPEs) and is used for space debris and minor planets measurements, namely for astrometry and photometry. IPEs consist from state of the art, as well as from our algorithms. Majority of the code was programmed by FMPI CU, except for several key libraries, such as Astrometry.net suite. Each IPE was individually validated as presented in this work. Thanks to the robust algorithms, astrometric and photometric reductions can be performed also on more challenging images, e.g., images with streaks. Validation revealed that the astrometric solution for different type of images reaches accuracy of around 1 arcsec which is highly satisfactory for defined purpose.

Our next step is to validate the image processing pipeline as a whole on a different type of observations, e.g., Near Earth Asteroids (NEA), Global Navigation Satellite System (GNSS), GEO and GTO or the very challenging Low Earth Orbit (LEO) objects observations. Additionally, because there are several heterogeneous optical sensors operated by the FMPI CU, we will investigate the possibility to use our developed pipeline on other systems too.

ACKNOWLEDGMENTS

The presented work was performed under a programme of ESA PECS activity "Development of a Supporting Optical Sensor for HAMR Objects Cataloguing and Research (HamrOptSen)", contract no. 4000117170/16/NL/NDe.

REFERENCES

1. Klinkrad, H. (2006). *Space Debris: Models and Risk Analysis*. 10.1007/3-540-37674-7.
2. T. Schildknecht, U. Hugentobler, A. Verdun, G. Beutler. (1995). *CCD Algorithms for Space Debris Detection, Final Report*. ESA/ESCO Contract No. 10623/93/IM
3. V. Kouprianov. (2008). *Distinguishing features of CCD astrometry of faint GEO objects*. Advances in Space Research. Volume 41, Issue 7, 2008, Pages 1029-1038. ISSN 0273-1177. <http://dx.doi.org/10.1016/j.asr.2007.04.033>.
4. Veres, P. et al. (2012). *Asteroid astrometry and photometry with trail fitting*. Publ. Astron. Soc. Pacific 124 (921), 1197–1207.
5. Silha et. al (2018). *Slovakian Optical Sensor for HAMR Objects Cataloguing and Research*. 69th International Astronautical Congress 2018 (IAC2018). Held 1-5 October 2018, in Bremen, Germany.
6. Karen A. Collins, John F. Kielkopf, Keivan G. Stassun, Frederic V. Hessman. (2016). *AstroImageJ: Image Processing and Photometric Extraction for Ultra-Precise Astronomical Light Curves*. arXiv:1601.02622, 10.3847/1538-3881/153/2/77
7. D. Lung et al. (2010). *Astrometry.net: Blind astrometric calibration of arbitrary astronomical reduction*. The Astronomical Journal, Volume 139, Number 5.
8. Raab H. (2012). *Astrometrica: Astrometric data reduction of CCD images*. Astrophysics Source Code Library, record ascl:1203.012.
9. Oda, H.; Kurosaki, H.; Yanagisawa, T.; Tagawa, M. (2014). *Optical observation, image-processing, and detection of space debris in geosynchronous Earth orbit*. 40th COSPAR Scientific Assembly. Held 2-10 August 2014, in Moscow, Russia. Abstract PEDAS.1-4-14.
10. Vallado et al. (2006). *Revisiting Spacetrack Report #3*. The AIAAAS Astrodynamics Specialist Conference. American Institute of Aeronautics and Astronautics, pp. 1-88.
11. Consultative Committee for Space Data Systems. (2017). *Tracking Data Message*. CCSDS 503.0-P-1.0.4, CCSDS. Pink Book, January 2017.